Influence of carbon nanotubes on the thermal, electrical and mechanical properties of poly(ether ether ketone)/glass fiber laminates

Díez-Pascual, Ana M.; Ashrafi, Behnam; Naffakh, Mohammed; González-Domínguez, José M.; Johnston, Andrew; Simard, Benoit; Martínez, M. Teresa; Gómez-Fatou, Marián A.

Publisher's version / Version de l'éditeur:
https://doi.org/10.1016/j.carbon.2011.03.011
Carbon, 49, 8, pp. 2817-2833, 2011-03-09

CARBON 49 (2011) 2817–2833

available at www.sciencedirect.com

ScienceDirect

journal homepage: www.elsevier.com/locate/carbon

Influence of carbon nanotubes on the thermal, electrical and mechanical properties of poly(ether ether ketone)/glass fiber laminates

Ana M. Díez-Pascual [a,*], *Behnam Ashrafi* [b], *Mohammed Naffakh* [a], *José M. González-Domínguez* [c], *Andrew Johnston* [b], *Benoit Simard* [d], *M. Teresa Martínez* [c], *Marián A. Gómez-Fatou* [a]

[a] *Department of Polymer Physics and Engineering, Institute of Polymer Science and Technology (CSIC), Juan de la Cierva 3, 28006 Madrid, Spain*

[b] *Institute for Aerospace Research, NRC, 1200 Montreal Road, Ottawa, Canada*

[c] *Department of Nanotechnology, Institute of Carbon Chemistry (CSIC), Miguel Luesma Castan 4, 50018 Zaragoza, Spain*

[d] *Steacie Institute for Molecular Sciences, NRC, 100 Sussex Drive, Ottawa, Canada*

ARTICLE INFO

Article history:
Received 26 October 2010
Accepted 2 March 2011

ABSTRACT

Novel poly(ether ether ketone) (PEEK)/single-walled carbon nanotube (SWCNT)/glass fiber laminates incorporating polysulfone as a compatibilizing agent were fabricated by melt-blending and hot-press processing. Their morphology, mechanical, thermal and electrical properties were investigated and compared with the behavior of similar non-compatibilized composites. Scanning electron micrographs demonstrated better SWCNT dispersion for samples with polysulfone. Thermogravimetric analysis indicated a remarkable improvement in the thermal stability of PEEK/glass fiber by the incorporation of SWCNTs wrapped in the compatibilizer, ascribed to a significant thermal conductivity enhancement. Differential scanning calorimetry showed a decrease in the crystallization temperature and crystallinity of the polymer with the addition of both wrapped and non-wrapped SWCNTs. The laminates exhibit anisotropic electrical behavior; their conductivity out-of-plane is lower than that in-plane. Dynamic mechanical studies revealed an increase in the storage modulus and glass transition temperature in the presence of polysulfone. Mechanical tests demonstrated significant enhancements in stiffness, strength and toughness by the incorporation of wrapped nanofillers, whilst the mechanical properties of non-compatibilized composites only improved marginally. Samples with laser-grown SWCNTs exhibit enhanced overall performance. This investigation confirms that SWCNT-reinforced PEEK/glass fiber compatibilized composites possess excellent potential to be used as multifunctional engineering materials in industrial applications.

1. Introduction

Conventional carbon fiber or glass fiber-reinforced polymer composites have been developed during the last decades to provide a wide range of materials which combine high stiffness and strength with low density. This combination of properties makes these materials particularly attractive for many applications in aerospace [1], automotive [2] and the

* *Corresponding author:* Fax: +34 915 644 853.
E-mail address: adiez@ictp.csic.es (A.M. Díez-Pascual).

0008-6223/$ - see front matter
doi:10.1016/j.carbon.2011.03.011

energy sector, both in alternative energy, e.g. wind turbine blades [3], and conventional energy generation, e.g. underground oil-drilling [4]. However, the potential use of these composites is in some cases hindered by poor out-of-plane properties, particularly delamination resistance. Two key factors contributing to poor resistance to delamination are weak fiber/matrix interfaces and the brittle nature of many polymer matrices. To address this problem, different through-thickness reinforcing elements such as 3D textiles or stitching [5] have been employed. However, these modifications of the composite structure improve neither the intrinsic interface nor the matrix properties. These issues must instead be addressed on the nanoscale, through surface modification of the fibers and/or toughening of the matrix. Carbon nanotubes (CNTs) have demonstrated outstanding mechanical, electrical and thermal properties [6], which combined with their high aspect ratio and nanoscale dimensions make them promising candidates to be used as nanofillers in polymer composites, opening up new perspectives for the development of the next generation of high-performance multifunctional materials for aerospace and terrestrial applications. Some efforts have been made to integrate CNTs into traditional fiber/polymer composites [7], by either dispersing the CNTs in the bulk of the matrix [8] or growing them onto the surface of the fibers [9,10]. In both cases, delamination resistance increases in comparison to conventional fiber-reinforced laminates due to different mechanisms of interaction between the propagating cracks and the CNTs, such as localized inelastic matrix deformation and void nucleation, CNT debonding, crack deflection, crack pinning, CNT pull-out, etc. [11]. Furthermore, the inclusion of CNTs generally improves the thermo-mechanical properties of the composite, increasing the glass transition temperature (T_g) of the matrix and decreasing its coefficient of thermal expansion [8]. The aforementioned techniques to develop "multiscale" materials have been explored primarily for carbon fiber-reinforced composites, and only a few studies have been reported on the effect of adding CNTs to glass fiber-reinforced composites [8,12–16]. It should also be noted that, to date, most of the literature related to these composites refers to thermoset matrices, which are usually prepared by direct infusion of the CNT/polymer resin into the glass fabric through vacuum-assisted resin transfer molding (VARTM) [17] method. However, it is still a big challenge to effectively manufacture CNT-reinforced thermoplastic laminates due to their high viscosity. Hence, investigation of the properties of this type of composite is limited.

Poly(ether ether ketone) (PEEK) is a high-performance semicrystalline thermoplastic that displays a unique combination of thermal stability, chemical inertness, high wear resistance and friction coefficient, excellent mechanical properties over a wide temperature range and low flammability [18]. This polymer can be processed by conventional techniques, such as extrusion and compression molding, and can be employed as matrix resin for reinforced composites. Since its commercialization, PEEK has been used in a wide range of applications, from medicine to the electronics, telecommunication and transportation industries (automobiles, aircraft and aerospace) [19]. For example, in space applications, this material is sometimes employed as a replacement for aluminum because of its superior performance at high temperatures. To extend its structural applications, several studies have been devoted to enhance the properties of PEEK via incorporation of fillers such as glass fibers [20–22] and carbon fibers [23,24]. Recently, our group has demonstrated that the properties of this high-performance material can be significantly enhanced by the addition of single-walled carbon nanotubes (SWCNTs) [25,26]. In particular, the addition of small amounts of SWCNTs wrapped in compatibilizing agents such as polysulfone, an amorphous thermoplastic miscible with and structurally similar to PEEK, leads to a remarkable increase in the storage and Young's modulus, T_g and degradation temperatures of the matrix [27,28]. Polysulfone possesses dual affinity with PEEK and the SWCNTs; its phenyl moieties interact with the matrix through π–π stacking as well as with the sp^2-bonded hexagonal networks of the nanofillers. Furthermore, chemical interaction of polar segments of the compatibilizer (sulfone, ether, etc.) to surface groups located on the SWCNT structure and defect sites (side-walls or open ends) boosts the compatibilization effect, leading to composites with enhanced nanofiller dispersion and CNT-polymer load transfer; as a result, the mechanical properties of these composites are superior to those containing pristine CNTs.

In the present work, SWCNT-reinforced PEEK/glass fiber laminates have been successfully manufactured through simple melt-blending and hot-press processing. These techniques are environmentally friendly and easy to scale up, which is of great interest for potential industrial applications. The developed hybrid composites consist of alternating layers of PEEK/SWCNT films and glass fabric plies, combining the properties of all the constituents; hence, they are expected to have improved performance in comparison with binary composites. SWCNTs were synthesized by two different methods (arc-discharge and laser) and then wrapped in polysulfone as a compatibilizing agent. The influence of SWCNT concentration and type as well as the presence of the compatibilizer on the electrical, thermal and mechanical performance of these multifunctional PEEK based laminates is discussed.

2. Experimental

2.1. Materials

The polymer (PEEK 150PF) was supplied in fine powder form by Victrex plc, UK ($M_w \sim 40{,}000$ g/mol, $T_g = 147$ °C, $T_m = 345$ °C, $d_{25°C} = 1.30$ g/cm^3, $\eta_{350°C} \sim 10^3$ Pa s). Arc and laser-grown SWCNTs were synthesized following the procedures reported in our previous works [25,26]. The compatibilizing agent poly(1–4-phenylene ether-ether sulfone), PEES ($M_w \sim 38{,}000$ g/mol, $T_g = 192$ °C, $d_{25°C} = 1.38$ g/cm^3), was provided by Sigma–Aldrich in pellet form. The SWCNTs were wrapped by this amorphous polymer in 1-methyl-2-pyrrolidone (NMP) solution. A detailed description of the wrapping process in liquid media is provided in a previous publication [27]. The amount of compatibilizer retained by the SWCNTs was determined by TGA analysis and was found to be ~11.2 and 8.5% for arc and laser-grown SWCNTs, respectively. The E-glass plain weave fiber fabric (TG09P) used in this work was purchased from JB Martin, Canada. It had an areal density of 0.0282 g/cm^2,

$d_{25°C}$ = 2.50 g/cm^3, and consists of bundles of microfibers (tows) with a single fiber diameter of ~12 μm.

2.2. Manufacturing of PEEK/SWCNT/ glass fiber laminates

Prior to compounding, PEEK powder and the SWCNTs were placed in an oven at 140 °C for 24 h to remove absorbed moisture. After drying, the polymer (~50 g) was physically mixed with the different types of SWCNTs, both wrapped and non-wrapped in PEES. Each mixture of PEEK/SWCNT (1.0 or 0.5 wt%) was then dispersed in 50 mL of ethanol and sonicated in an ultrasonic bath for 30 min. Subsequently, the dispersion was partly dried under vacuum (70 mbar) at 50 °C for 5 min, sonicated for another 30 min and heated until total evaporation of the solvent. The melt-compounding of the resulting solid dispersions was performed in a Haake Rheocord 90 extruder operating at 380 ± 5 °C, with a rotor speed of 150 rpm, using mixing times of 20 min. About 5.7 g of the extruded PEEK/SWCNT was used to fabricate films with a thickness of ~0.5 mm. A brass picture frame was employed to control the dimensions. Two flat brass plates were used as top and bottom surfaces to guarantee uniform thickness of the thin films. A Kapton layer was placed between each brass plate and the PEEK/SWCNT mixture to avoid adhesion of the material to the plates (Fig. 1a). The films were made using a hot-press at 380 °C, under successive pressure dwells of 5, 40 and 130 bars, for periods of 6 min at each pressure.

The laminates were prepared by alternatively placing 4 plies of glass fabric within 5 PEEK/SWCNT films; the schematic representation of the lay-up stacking sequence is shown in Fig. 1b. Consolidation of the material was made at 380 ± 5 °C in a hot-press under high pressure. The heating rate to the dwell temperature was about 5 °C/min, with cooling to room temperature done slowly at a rate ⩽3 °C/min. The entire consolidation process cycle is displayed in Fig. 1c. The pressure steps were optimized to minimize the formation of internal pores and to improve fiber impregnation. The areal density of the glass fabric, the weight and lateral dimensions of the panels were used to determine the weight fraction of each constituent. The experimental density (ρ_c) of laminate coupons at 20 °C was accurately determined by the immersion technique, using a specific gravity determination kit. Taking into account the density of the fiber (ρ_f) and matrix (ρ_m), the theoretical density of the laminates was estimated using the equation [29]: $\rho_T = 100/[(w_m/\rho_m) + (w_f/\rho_f)]$. The void content was then calculated as difference between the experimental and the theoretical density [29]: Void content (%) = $[(\rho_T - \rho_c)/\rho_T] \times 100$. Subsequently, the corresponding volume fractions were obtained. The laminates had a matrix volume fraction of 51 ± 2%, a fiber volume fraction of 47 ± 1%, and an average void content <3%. Each composite panel exhibited a nominal thickness of 1 ± 0.1 mm, and was cut into test specimens with a Rockwell Delta band saw in a way that their edges followed the direction of the fibers (0° and 90°). To minimize the influence of the thickness variation, the data reported for each of the laminates correspond to the average of several specimens cut from different locations.

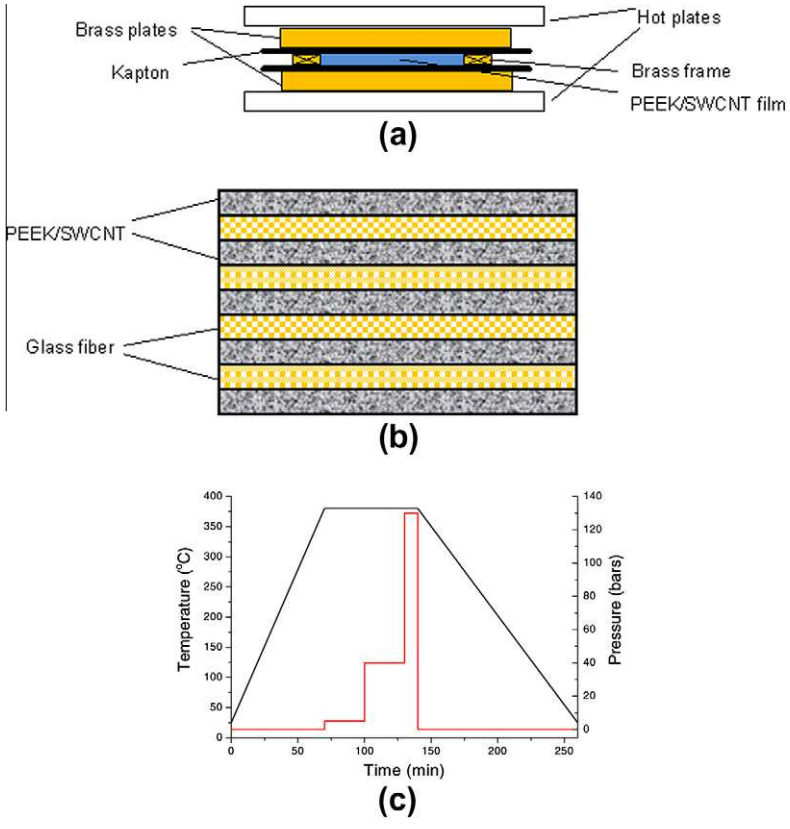

Fig. 1 – (a) Heated press used for the preparation of the PEEK/SWCNT films. (b) Schematic representation of the lay-up stacking sequence of the PEEK/SWCNT/glass fiber laminates. (c) Consolidation cycle used for laminate manufacturing.

2.3. Characterization techniques

2.3.1. Optical and scanning electron microscopies

Optical microscopy (OM) images at low magnification were obtained with a Nikon SMZ 1000 zoom stereomicroscope equipped with a plan 1X Ergo objective and a coaxial episcopic illuminator using a 12 V/150 W fiber optic light source. The microscope is coupled to a Pixelink camera model PL-A632 to capture and archive the digital images. The surface morphology of fractured specimens was analyzed with a Philips XL30 scanning electron microscope (SEM) applying an acceleration voltage of 25 kV and an intensity of 9×10^{-9} A. Laminate samples were coated with a ~5 nm Au/Pd overlayer in a Balzers SDC evaporator to avoid charge accumulation during electron irradiation.

2.3.2. Differential scanning calorimetry

Dynamic DSC experiments were conducted in a Mettler TA4000 differential scanning calorimeter, equipped with a DSC-30 oven with automatic temperature control, operating in a nitrogen environment. Samples of ~40 mg sealed in aluminum pans were heated to 380 °C for 5 min, cooled to ambient temperature and then reheated to 380 °C, all the steps at a constant rate of 10 °C/min. Glass transition temperatures were determined as the mid-point of the baseline shift, and the crystallization and melting temperatures were taken as the peak maxima or minima in the calorimetric curves. The crystallinities were estimated by the relation: $X_m = \Delta H_{m,\mathrm{PEEK}}/(\Delta H^{\circ}_{m,\mathrm{PEEK}} \times w_{\mathrm{PEEK}})$, where $\Delta H^{\circ}_{m,\mathrm{PEEK}}$ is the heat of fusion of an infinitely thick PEEK crystal (~130 J/g) [30], $\Delta H_{m,\mathrm{PEEK}}$ is the apparent melting enthalpy of PEEK and w_{PEEK} is the weight fraction of the polymer.

2.3.3. Thermogravimetric analysis

The thermal stability of the laminates and their residual weight were analyzed by thermogravimetric analysis (TGA) using a Mettler TA-4000/TG-50 thermobalance coupled to a mass spectrometer, at a heating rate of 10 °C/min. The temperature was scanned from room temperature to 800 °C under a dry air atmosphere. Experiments were carried out on samples with an average mass of 150 mg, and the purge air flow rate was 50 ml/min.

2.3.4. Electrical conductivity measurements

DC volume conductivity measurements were performed at ambient temperature using a source meter (Keithley 2635A). Both sample surfaces were covered by silver conductive epoxy paint electrodes to create non-guarded electrodes. The voltage applied to the samples was cycled 5 times in the range 0–20 V. The maximum voltage (20 V) was kept low to avoid melting or degrading the resin due to Joule heating. The measured current–voltage curves were linear (R^2 value > 0.9), and the resistance was obtained as the plot slope. The conductivity σ_v was calculated based on $\sigma_v = t/R_v \times A$, where A, t and R_v *are the area, thickness and volume resistance of the specimen, respectively. Volume conductivity was measured in both the through-thickness and in-plane directions. Note that* t is the thickness of the composite in the case of a through-thickness test, but it is the length for an in-plane resistivity measurement. For both directions, at least 3 specimens of each type of laminate were tested to get an average value.

2.3.5. Thermal conductivity measurements

The room temperature thermal diffusivity (α) of the composites was measured in the out-of-plane direction by a laser pulse method [31]. An Nd:YAG laser with wavelength of 1.06 μm was used to heat the front surface of the samples. An MCT (Mercury, Cadmium, Tellurium) infrared detector with response time of 40 ns and cutoff wavelength of 12.5 μm was employed for temperature measurement. The data were collected with a 500 M bandwidth TDS3052B oscillograph, and adjusted to fit the Clark–Taylor model. The measurement error of the system was below ±5% after calibration. The thermal conductivity was calculated according to the expression: $\lambda = \rho \times C_p \times \alpha$, where ρ is the density of the samples and C_p the specific heat capacity obtained from DSC measurements. At least 5 readings for each specimen were tested to report an average value.

2.3.6. Dynamic mechanical analysis

The dynamic mechanical performance of the samples was analyzed using a Mettler DMA 861 dynamic mechanical analyzer. Experiments were performed in tensile mode at frequencies of 0.1, 1 and 10 Hz. A dynamic force of 6 N was used oscillating at fixed frequency and amplitude of 30 μm. The relaxation spectra were recorded in the temperature range between −130 and 250 °C, at a heating rate of 2 °C/min.

2.3.7. Tensile and flexural tests

The tensile and flexural properties of the laminates were measured with an INSTRON 4204 mechanical tester at room temperature and 50 ± 5% relative humidity, using a crosshead speed of 1 mm/min and a load cell of 1 kN. Tensile specimens (Type V) and rectangular flexural coupons were employed, according to UNE-EN ISO 527-1 and 178 standards, respectively. All the samples were conditioned for 24 h before the measurements. The data reported are the average of the results for 5 specimens.

2.3.8. Charpy impact tests

Charpy notched impact strength measurements were carried out using a CEAST Fractovis dart impact tester. A hammer mass of 1.096 kg impacted at a constant velocity of 3.60 ms^{-1} (giving a total kinetic energy at impact of 7.10 J) on notched specimen bars with a V-shape notch tip radius = 0.25 mm, as described in the UNE-EN ISO 179 standard. Measurements were performed at 23 ± 2 °C and 50 ± 5% relative humidity. The presented data correspond to the average value of at least 6 specimens.

3. Results and discussion

3.1. Morphological observations

In order to assess the morphology and state of CNT dispersion of the fabricated laminates, the cross-sections of specimens cut from different locations were examined by OM and SEM, with typical images displayed in Fig. 2. As it can be observed

from OM images, all laminates exhibit a good degree of fiber impregnation, and a matrix-rich region is formed between glass plies. The fiber tows are rather wavy, since plain wave fabric was used for the manufacturing of the composites. Hence, it is difficult to estimate the average thickness of each ply within a laminate. Regarding SEM micrographs, the image of the reference PEEK/glass fiber (Fig. 2a, right) shows the glass fiber tows, with an average fiber diameter of 12 μm, surrounded by the PEEK polymer. The pore structure of the glass fabric is dual scale; the spacing between individual fibers within a tow (1–2 μm, see the inset in the micrograph) is about two orders of magnitude lower than that between the different fiber tows. Therefore, the permeability within the tows is much lower than between tows. The fibers are uniformly distributed through the polymer, and no open ring holes are found around them, indicative of the good fiber–matrix interfacial adhesion. The micrograph in Fig. 2b corresponds to a region between fiber tows of the laminate incorporating 1.0 wt% non-wrapped arc-SWCNTs, showing the existence of small CNT agglomerates (see the circle marked on the image). As can be visualized in the inset, the aggregates form a highly entangled interconnected structure, with SWCNT bundle diameters in the range 30–60 nm, values similar to those found previously for PEEK/arc-SWCNT composites [25]. These SWCNT aggregates (bigger than 2 μm) envelop the fiber tows but do not penetrate into them. The micrograph of the corresponding compatibilized sample (PEEK/arc (1.0 wt%) + PEES/glass fiber, Fig. 2c) displays a random and improved SWCNT dispersion; the addition of the polysulfone induced CNT disentanglement and disaggregation inside the polymer matrix, leading to a reduction in bundle size in comparison to the non-wrapped SWCNTs. According to the images, they have an average bundle diameter of ~35 nm (see the inset), and are preferentially located in matrix-rich regions or between fiber tows. No agglomerates or entanglements were observed in the examined regions, indicating larger effective contact

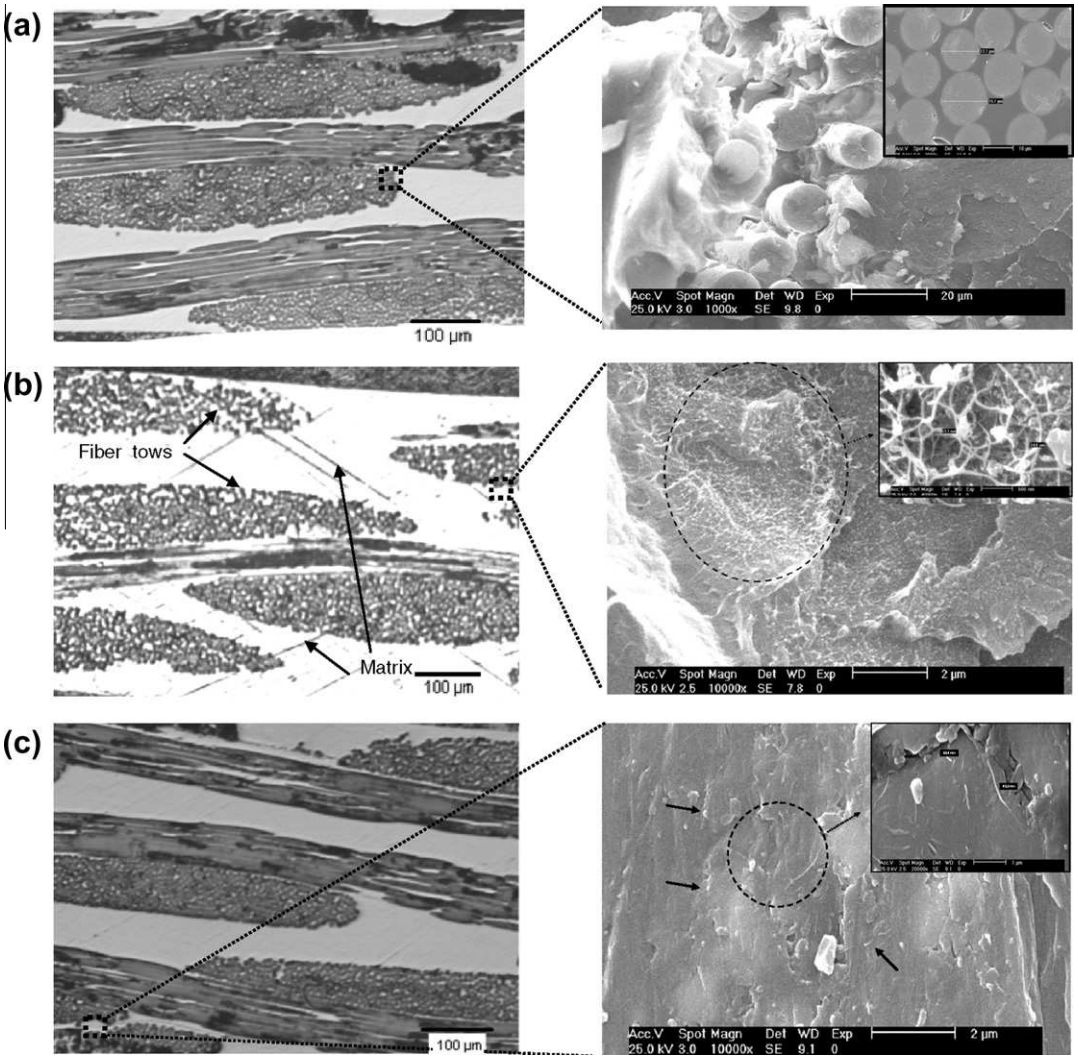

Fig. 2 – OM (left) and SEM (right) images obtained from the cross-section of different laminates: (a) PEEK/glass fiber; (b) PEEK/arc (1.0 wt%)/glass fiber; (c) PEEK/arc (1.0 wt%) + PEES/glass fiber. The images were obtained perpendicular to the plane of the glass fiber. SEM micrographs in (b) and (c) were taken from a region between the fiber tows. The dashed circle in (b) shows a small area of agglomerated SWCNTs in the non-compatibilized sample. The solid arrows in (c) point out randomly distributed nanotube bundles in the matrix.

area and thus stronger CNT–PEEK interfacial adhesion. Moreover, the isolated CNT bundles are expected to penetrate more easily within the glass fiber tows, leading to better fiber impregnation. The aforementioned observations are consistent with the results obtained from the comparative study of PEEK/SWCNT composites with and without compatibilizer [27], which revealed noticeably enhanced CNT dispersion for samples with PEES. This improvement is less significant at lower CNT loading, since the tendency to form agglomerates becomes stronger with increasing concentration. On the other hand, small differences were found between the morphology and state of nanofiller dispersion of laminates reinforced with laser or arc-SWCNTs, also in agreement with previous works [25,26].

3.2. *Crystallization and melting behavior*

It is well known that the crystallization process plays a crucial role in the properties of semicrystalline polymers. Therefore, it is important to analyze the influence of the SWCNTs and the glass fiber on the crystallization and melting behavior of PEEK. The DSC cooling and melting curves of the different manufactured laminates are displayed in Fig. 3, and the calorimetric parameters derived from the thermograms are collected in Table 1. The crystallization temperature (T_c) (~309 °C for pure PEEK [25]) drops about 5 °C for the reference laminate. In the compatibilized samples including 1.0 wt% laser and arc-SWCNT loading, the decrease in comparison to the reference is ~9 and 7 °C, respectively (Fig. 3a), whilst the addition of similar amounts of non-wrapped SWCNTs only lowers T_c by ~5 and 4 °C. Nevertheless, the sample including 0.5 wt% wrapped laser SWCNTs shows similar T_c to PEEK/glass fiber. On the other hand, the level of crystallinity (X_c) falls slightly (~8%) for the reference laminate in comparison to that of PEEK. Composites including 1.0 wt% SWCNTs exhibit an additional crystallinity decrease (~3% and 5% for wrapped and non-wrapped nanofillers, respectively), whilst for those incorporating 0.5 wt% SWCNT loading, X_c is approximately maintained. Actually, there are two factors controlling the crystallization of polymeric composite systems. One is that fillers may have a nucleating effect, which results in higher T_c. The other is that they hinder the diffusion and migration of polymer chains, which inhibits crystallization. In the case of PEEK/glass fiber, the second effect is probably dominant, thereby leading to lower X_c and T_c. This is in contrast with the results reported for 30% short glass-fiber reinforced PEEK composites prepared by injection moulding [21], where the fibers act as nucleating agents that increase the degree of crystallinity of the matrix. The discrepancy could be explained based on the different attributes of the fillers (mainly size and aspect ratio) and the manufacturing processes. On the other hand, the addition of SWCNTs is likely two fold due to the competition of the above mentioned factors. When 0.5 wt% SWCNT content is incorporated in the reference laminate, the nucleating effect probably compensates for restrictions in chain mobility; hence T_c and X_c remain unchanged. However, at higher loadings, although the nucleation surface becomes larger, the formation of a strong CNT network hinders the crystal growth, leading to slightly lower T_c and X_c for these composites. Comparison of the results obtained for compatibilized and non-compatibilized laminates suggests that the effect of confinement of the polymer chains becomes stronger in the presence of the compatibilizing agent, which is reasonable considering that PEES is an amorphous polymer miscible with the matrix which inhibits its crystallization process. Moreover, the polysulfone promotes interfacial CNT-polymer adhesion. Although the wrapped nanofillers are better dispersed within the matrix, which would accelerate the nucleation process, the additional interactions result in more hindrance to the diffusion of the polymer chains; overall, the crystallization process is slowed in comparison with composites including non-wrapped SWCNTs. Analogous inhibitory effects on polymer mobility for crystallization caused by enhanced interactions between modified nanotubes and polymer matrices have been reported in the literature for poly(ethylene oxide) [32] and polyamide [33] composites. Regarding the influence of the nanofiller type, it is found that laminates with arc-purified SWCNTs possess slightly higher T_c and X_c than those reinforced with laser SWCNTs. This is consistent with observations made from the X-ray diffractograms of the wrapped SWCNTs [27], which indicated that arc-SWCNTs dispersed in PEES are more effectively disentangled and debundled.

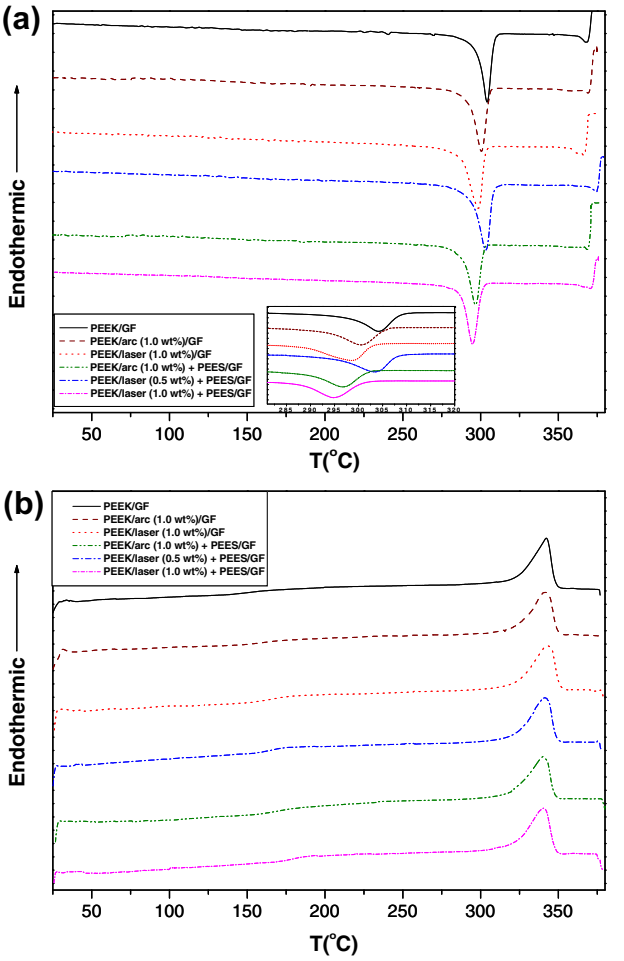

Fig. 3 – Non-isothermal DSC curves for PEEK laminates at a rate of 10 °C/min. (a) Cooling scans; (b) heating scans. To simplify the nomenclature, GF denotes glass fiber.

Table 1 – DSC thermal parameters for the manufactured PEEK/SWCNT/glass fiber laminates. For comparison, data for pure PEEK taken from Ref. [25] are also included in the table. To simplify the nomenclature, GF denotes glass fiber.

Sample (% SWCNTs)	T_c (°C)	X_c (%)	T_m (°C)	X_m (%)	T_g (°C)
PEEK	309.0 ± 0.3	43 ± 1	344.2 ± 0.5	45 ± 1	147 ± 1
PEEK/GF	304.2 ± 0.5	39 ± 1	342.2 ± 0.7	42 ± 1	156 ± 2
PEEK/arc (1.0 wt%)/GF	300.1 ± 0.8	38 ± 2	341.7 ± 0.8	40 ± 2	161 ± 1
PEEK/laser (1.0 wt%)/GF	298.7 ± 0.7	38 ± 1	342.6 ± 0.6	41 ± 1	167 ± 2
PEEK/laser (0.5 wt%) + PEES/GF	303.5 ± 0.8	40 ± 1	341.5 ± 0.6	43 ± 1	165 ± 3
PEEK/arc (1.0 wt%) + PEES/GF	296.6 ± 0.5	37 ± 1	339.8 ± 0.8	40 ± 1	173 ± 2
PEEK/laser (1.0 wt%) + PEES/GF	294.8 ± 0.6	36 ± 2	340.4 ± 0.7	39 ± 1	178 ± 1

T_c and T_m are the crystallization and melting temperatures, respectively. X_c and X_m correspond to the crystallization and melting crystallinities. T_g is the glass transition temperature obtained from the heating thermograms.

Focusing on the heating scans (Fig. 3b), it can be observed that the melting temperature (T_m) (~344 °C for PEEK) shows small changes with the inclusion of the glass fiber or the SWCNTs. Thus, T_m of PEEK/glass fiber is around 342 °C and that of laminates including 1.0 wt% wrapped SWCNTs are around 340 °C. Moreover, the degree of crystallinity (X_m) obtained from the heating thermograms decreases slightly in the presence of both fillers, showing similar trends to those described previously for X_c. As mentioned earlier, the incorporation of reinforcing elements hampers chain motion, making the crystallization process more difficult; this inhibits molecular packing, resulting in the formation of smaller and less perfect crystals, which have lower T_m. Overall, differences among the levels of crystallinity of the various laminates are relatively small, lower than 7%; similar observations were found from the previous comparative study of PEEK/SWCNT composites with and without compatibilizer [27].

On the other hand, the heating thermograms show a small variation of the heat capacity related to the glass transition process. This transition temperature (T_g) rises with the inclusion of the glass fiber and the SWCNTs (Table 1). For the reference composite T_g is about 156 °C (~9 °C higher than pure PEEK) and it further increases about 20 °C in the laminate with 1.0 wt% wrapped laser SWCNTs, which is consistent with the restrictions on mobility imposed by the CNT-polymer interactions and the decrease in crystallinity observed for these laminates. T_g values for the different samples have been more accurately determined from the dynamic mechanical spectra and will be discussed in a following section.

3.3. *Electrical conductivity measurements*

Traditional glass fiber-reinforced composites are electrically insulating, which sometimes limits their use in the electronics and aerospace industries, since an electrical conductivity greater than 10^{-8} S/cm is required to prevent the buildup of static charge [34]. The incorporation of small amounts of CNTs as conductive fillers opens up the possibility for the development of new multifunctional materials with improved electrical performance. Their conductive properties depend strongly on the concentration, aspect ratio and dispersion degree of the CNTs, as well as filler–matrix and filler–filler interfacial interactions [35]. To analyze the influence of these parameters and the compatibilizer on the electrical conductivity (σ) of the fabricated laminates, room temperature measurements were performed both in the in-plane and through-thickness directions, and the results are plotted in Fig. 4. Both pure PEEK and PEEK/glass fiber composite are insulating materials ($\sigma < 10^{-13}$ S/cm), and become semiconducting with the addition of the SWCNTs. This means that the SWCNT volume fraction exceeds the percolation threshold, the concentration at which electrically conductive networks of CNTs are formed. Such a low percolation threshold (<0.5 wt%) is indicative of the good CNT dispersion attained in these laminates. The conductivity in-plane was in the range 10^{-6}–10^{-4} S/cm, which was about one order of magnitude higher than that out-of-plane. Similar anisotropic electrical behavior has been observed for polyethylene [35] and epoxy [9] multiscale composites. This observation is explained by the fact that the glass fiber orientation in-plane inhibits the formation of electrical conductive paths in the z-direction. This behavior could also be related to the processing of the laminates; considering that the pressure was applied in direction perpendicular to the glass plies, the SWCNTs might be preferentially aligned along the resin flow direction.

With regards to the effect of CNT content, it was found that σ increases only about one order of magnitude when

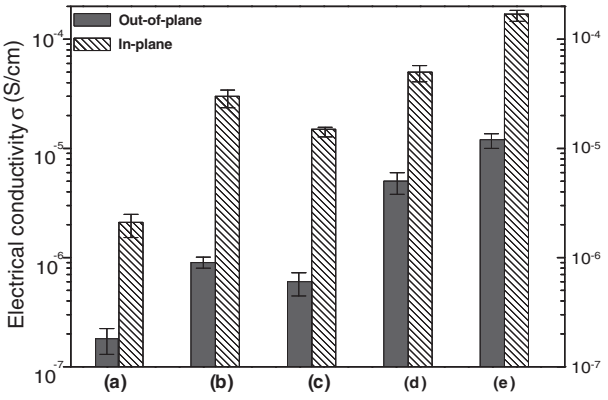

Fig. 4 – DC in-plane and out-of-plane electrical conductivity of PEEK based laminates at room temperature: (a) PEEK/arc (1.0 wt%)/glass fiber; (b) PEEK/laser (1.0 wt%)/glass fiber; (c) PEEK/laser (0.5 wt%) + PEES/glass fiber; (d) PEEK/arc (1.0 wt%) + PEES/glass fiber; (e) PEEK/laser (1.0 wt%) + PEES/glass fiber.

the concentration rises from 0.5 to 1.0 wt%, as expected since these weight fractions are above the percolation threshold. However, the quality, aspect ratio and state of dispersion of the nanofillers play a more important role on the electrical behavior. For both studied directions, laminates reinforced with laser-grown SWCNTs exhibit enhanced conductivity, probably related to the lower defect content of this type of nanofiller. The purification treatment could have induced small defects on the CNT side-walls, which would have detrimental effects on the conductivity. Thus, the inclusion of 1.0 wt% non-wrapped arc-purified SWCNTs increases the in-plane conductivity by about seven orders of magnitude in comparison to the pure resin, whilst the addition of similar amount of laser-grown SWCNTs raises conductivity by around eight orders of magnitude. The influence of the compatibilizer seems to be two fold. On one hand, it leads to a better and more stabilized dispersion of the SWCNTs due to improved intermolecular interactions with the PEEK matrix, which would enhance the electron charge transfer in these samples. On the other hand, it is widely accepted that polymer wrapping increases tube-tube resistance, thereby leading to a reduction in conductivity. It appears that the disadvantages of the compatibilization with respect to SWCNT conductivity are outweighed by the enhanced dispersion and adhesion attained in the presence of the polysulfone; overall, the electrical conductivity attained in the laminates reinforced with wrapped SWCNTs is on average one order of magnitude higher than that obtained for the non-compatibilized samples. This is in contrast with the results obtained from the previous study of PEEK/SWCNT composites [28], where the incorporation of the compatibilizer maintained the level of conductivity of the samples. The discrepancy could be attributed to the influence of additional factors, such as the presence of nanoscale pores. According to SEM observations, non-compatibilized laminates have small CNT agglomerates, which could obstruct the diffusion of the matrix during processing. This may result in very small voids [17] which would interrupt conductive pathways, thereby reducing overall conductivity. The best electrical properties are found for the laminate including laser-SWCNTs wrapped in PEES, in which the in-plane conductivity increases by about nine orders of magnitude in comparison to the pure resin. It is important to notice that this improvement is the consequence of different synergic effects, mainly enhanced impregnation, quality and dispersion of the SWCNTs.

3.4. *Thermal conductivity measurements*

The performance of advanced multifunctional materials is highly dependent on the effective dissipation of accumulated heat. Composites with good thermal conductivity have a great number of potential applications such as printed circuit boards, connectors, thermal interface materials, heat sinks, etc. The thermal conductivity (λ) of neat PEEK resin is $\sim$0.23 W m^{-1} K^{-1} [28], and that of glass fiber fabric around 0.05 W m^{-1} K^{-1} [36]. Phonon transport in these composites is in the form of diffusion, and since CNTs exhibit ballistic transport properties [37], the dispersion of CNTs into the matrix will significantly enhance phonon diffusion, thereby improving thermal conductivity. The room temperature out-of-plane thermal conductivity values of the different manufactured composites are shown in Fig. 5. λ of the reference material is about 0.22 W m^{-1} K^{-1}, very close to that of the pure resin. The addition of 1.0 wt% non-wrapped arc and laser-grown SWCNTs increases this value by about 18% and 53%, respectively, whilst for the corresponding compatibilized samples the increments are $\sim$32% and 90%. This indicates that the thermal conductivity is also sensitive to the attributes of the nanofiller (aspect ratio, presence of defects and content in metal impurities) as well as to the presence of the compatibilizer that influences the degree of dispersion. Despite the wrapping in the polysulfone hinders the direct contact among the tubes, which would lower the thermal conductivity, it improves the distribution of the SWCNTs and their adhesion with the matrix; overall, samples with PEES exhibit higher λ values than the non-compatibilized. With regards to the type of nanotube, it is again found that laminates incorporating laser-grown SWCNTs exhibit enhanced conductivity. Moreover, λ is also found to rise with increasing CNT content, and experiences about 50% enhancement when the concentration is doubled. Wang and Qiu [36] investigated the thermal conductivity of polyester/vinyl ester resin/MWCNT/GF composites, and reported λ improvements of 67% and 150% for 1 and 3 wt% MWCNT contents respectively. Assael and co-workers [38], dealing with epoxy/MWCNT/GF composites found a maximum λ enhancement of 60% at 1.2 wt% loading. The increment attained in our laminate incorporating 1.0 wt% laser-SWCNTs dispersed in PEES is close to 100%, attesting to the high quality of this sample. If more SWCNTs could be uniformly incorporated into the polymer matrix, more significant enhancement would be achieved.

For polymer/CNT/GF multiphase laminates, the thermal conductivity can be predicted with a two-phase model. Firstly, according to the research of Patton et al. [39], λ of polymer/CNT composites can be assumed to follow the modified rule of mixture for discontinuous reinforcement: $\lambda_c = \eta_l^2 \lambda_f V_f + \lambda_m(1 - V_f)$, where λ_f and λ_m are the thermal conductivity of

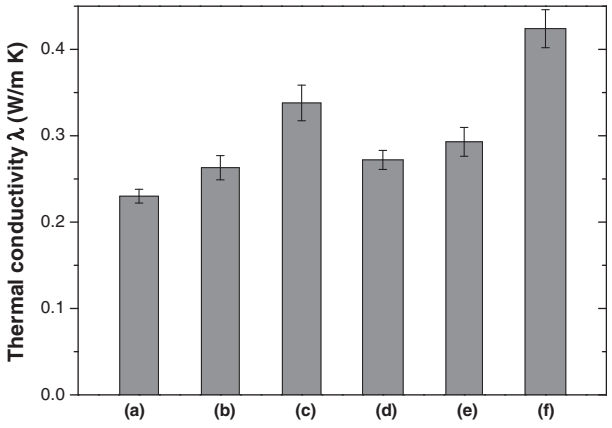

Fig. 5 – Room temperature out-of-plane thermal conductivity values of the different PEEK laminates: (a) PEEK/glass fiber; (b) PEEK/arc (1.0 wt%)/glass fiber; (c) PEEK/laser (1.0 wt%)/glass fiber; (d) PEEK/laser (0.5 wt%) + PEES/glass fiber; (e) PEEK/arc (1.0 wt%) + PEES/glass fiber; (f) PEEK/laser (1.0 wt%) + PEES/glass fiber.

the filler and the matrix, V_f the filler volume fraction and η_l the length efficiency factor that accounts for the waviness of the CNTs, which was assumed to be 0.2 [39]. Dispersion of the CNTs into the polymer results in a new matrix phase with improved properties, and fibers can now be regarded as the filler phase; the rule of mixtures can be subsequently used to calculate λ of the laminates. Taking into account the exceptionally high thermal conductivity of SWCNTs ($\sim$2000 W m^{-1} K^{-1}) [40], the improvements in λ observed in these laminates are considerably below those expected according to the engineering rule of mixtures (0.35 and 0.56 for 0.5 and 1.0 wt% CNT content). Samples including laser-grown SWCNTs dispersed in PEES show the smallest deviations with respect to the predictions (differences of 22% and 25% for 0.5 and 1.0 wt% loadings). The discrepancies between the theoretical and experimental values could be attributed to the low thermal conductance of the CNT–polymer interface and the high interfacial thermal resistance between SWCNTs [41], which considerably limit heat transfer. These observations are consistent with the low thermal conductivity of SWCNT film (buckypaper)/PEEK laminates as compared to theoretical predictions [42]. Future work is likely to improve these results by the introduction of covalent bonds between the SWCNTs and the polymer matrix, since it has been reported [43] that the presence of chemical bonding reduces the tube–matrix thermal interfacial resistance.

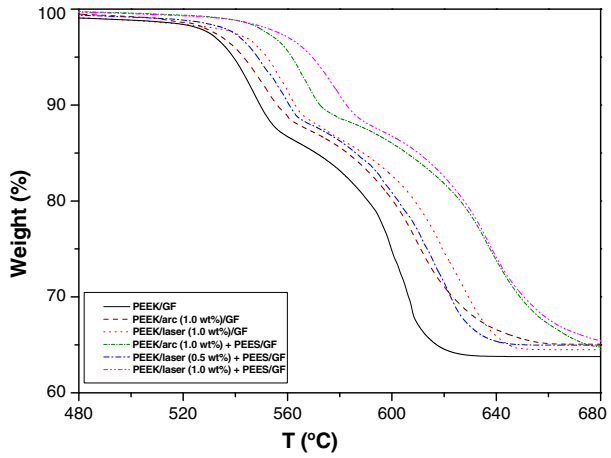

Fig. 6 – TGA curves for the PEEK based laminates obtained under dry air atmosphere at a heating rate of 10 °C/min. For comparative purposes, only the temperature range between 480 and 680 °C is plotted.

3.5. *Thermal stability*

The thermal stability of polymer composites depends on morphological factors, such as size, degree of dispersion of the filler and level of interfacial adhesion with the matrix, and is also influenced by the composition. To evaluate the effect of these parameters on the stability of the PEEK laminates, TGA experiments were carried out under dry air atmosphere, and the corresponding thermograms are depicted in Fig. 6; the characteristic degradation temperatures of the different samples are collected in Table 2. All the laminates display two degradation steps, similarly to pure PEEK, the first related to the scission of the polymeric chains and the second to the degradation of the ether and aromatic structures [25]. Their residual weight at 700 °C is in good agreement with their glass fiber content. Pure PEEK starts to degrade (T_i) around 480 °C and shows maximum rates of weight loss (T_{max1} and T_{max2}) at 530 and 584 °C, respectively. As expected, the incorporation of the glass fiber delays the degradation process of the matrix, increasing T_i and both T_{max} by about 40 and 20 °C, respectively; this is in agreement with the results reported for composites based on other thermoplastic matrices such as glass fiber-reinforced polycarbonate (PC)/acrylonitrile–butadiene–styrene (ABS) blends [44]. Regarding the different laminates, higher degradation temperatures are found for samples with PEES. Thus, for the compatibilized composite including 1.0 wt% laser SWCNTs, T_i, T_{max1} and T_{max2} rise by $\sim$34, 30 and 40 °C, respectively, in comparison with the reference laminate, whereas for the analogous non-compatibilized samples the increments are only 9, 12 and 22 °C. The polysulfone improves the dispersion of the nanofillers and enhances their adhesion with the polymer matrix; this should increase the barrier effect of the SWCNTs, which effectively hinder the diffusion of degradation products from the bulk of the polymer to the gas phase, hence slowing down the decomposition process. Analogous behavior was found from a comparison of the TGA thermograms of PEEK/SWCNT composites with and without compatibilizer [27]. With increasing CNT loading,

Table 2 – Characteristic degradation temperatures of PEEK laminates obtained from TGA measurements under dry air atmosphere at a heating rate of 10 °C/min.

Sample (% SWCNTs)	T_i (°C)	T_{10} (°C)	T_{max1} (°C)	T_{max2} (°C)	ΔT (°C)
PEEK	478 ± 1	520 ± 1	530 ± 1	584 ± 1	54 ± 1
PEEK/GF	516 ± 1	548 ± 2	547 ± 1	602 ± 2	55 ± 3
PEEK/arc (1.0 wt%)/GF	523 ± 2	555 ± 1	553 ± 1	611 ± 1	58 ± 2
PEEK/laser (1.0 wt%)/GF	525 ± 1	562 ± 1	559 ± 2	624 ± 2	65 ± 4
PEEK/laser (0.5 wt%) + PEES/GF	519 ± 1	558 ± 1	556 ± 1	618 ± 2	60 ± 3
PEEK/arc (1.0 wt%) + PEES/GF	547 ± 2	571 ± 1	569 ± 1	640 ± 1	69 ± 2
PEEK/laser (1.0 wt%) + PEES/GF	550 ± 1	582 ± 1	577 ± 2	642 ± 1	64 ± 2

T_i is the initial degradation temperature obtained at 2% weight loss. T_{10} is the temperature corresponding to 10% weight loss. T_{max} is the maximum degradation rate temperature; the subscripts 1 and 2 refer to the first and second degradation stages, respectively. ΔT is the difference between T_{max1} and T_{max2}.

the barrier effect becomes stronger, which is reflected in higher degradation temperatures.

Focusing on the influence of the nanofiller type, better thermal stability is observed for laminates including laser-grown SWCNTs. For the same CNT content, T_i, T_{max1} and T_{max2} of samples reinforced with arc-purified SWCNTs are on average 2, 6 and 10 °C lower than those including laser SWCNTs. This is in contrast with the results obtained from the previous study of the PEEK/SWCNT composites [26], where samples with arc-purified SWCNTs exhibited the highest decomposition temperatures, ascribed to the lower metal content of this type of nanofiller. However, in the case of the laminates, the thermal stability seems to be directly related to the effect of higher thermal conductivity that facilitates heat dissipation within the sample; as mentioned previously, laminates reinforced with wrapped laser-grown SWCNTs exhibit the highest thermal conductivity values. On the other hand, the difference between T_{max1} and T_{max2} (ΔT) is on average 10 °C higher for the SWCNT-reinforced laminates in comparison with the reference, which indicates that with the addition of the nanofillers, the scission of the polymer chains takes places over a longer period of time. Overall, TGA results confirm that these laminates are suitable for use in high-temperature applications.

3.6. Dynamic mechanical properties

DMA tests were performed to monitor changes in the stiffness of the composites as a function of temperature. Dynamic mechanical tests over a wide range of temperature and frequency are sensitive to several transitions and relaxation processes of the resin in the composite, and provide information about the fiber–matrix and CNT–matrix interfaces. Fig. 7a shows the temperature dependence of the storage modulus (E') at a frequency of 1 Hz. E' values for the different laminates at 25, 100 and 200 °C are collected in Table 3. The storage modulus is indicative of the elastic energy stored in the material, and is highly affected by its composition, morphology and geometric characteristics. At room temperature, E' of pure PEEK is around 3.8 GPa [25]; the inclusion of the glass fiber results in a 3.4-fold improvement in modulus, indicating effective stress transfer from the matrix to this reinforcement. Similar E' enhancement has been reported for other glass-fiber reinforced composites such as PC/ABS blends [44]. Regarding the different laminates, significantly larger E' increments are found for samples incorporating wrapped SWCNTs. At 25 °C, the inclusion of 1.0 wt% non-wrapped arc and laser-grown SWCNTs only produces an increase in the modulus of PEEK/glass fiber of 5% and 8%, respectively, whilst the addition of similar amount of nanotubes dispersed in PEES raises E' by an average of 18% and 21%. Similar trends were found for E' values at 100 °C. The differences between compatibilized and non-compatibilized composites probably arise from several factors. Firstly, the wrapped SWCNTs are better dispersed within the matrix, allowing a more uniform load distribution. Secondly, the compatibilizer improves the CNT–PEEK interfacial adhesion, which enables a more efficient stress transfer. In contrast, as revealed by SEM analysis, the non-compatibilized composites exhibit bigger SWCNT bundle size and even some agglomerates, which are known

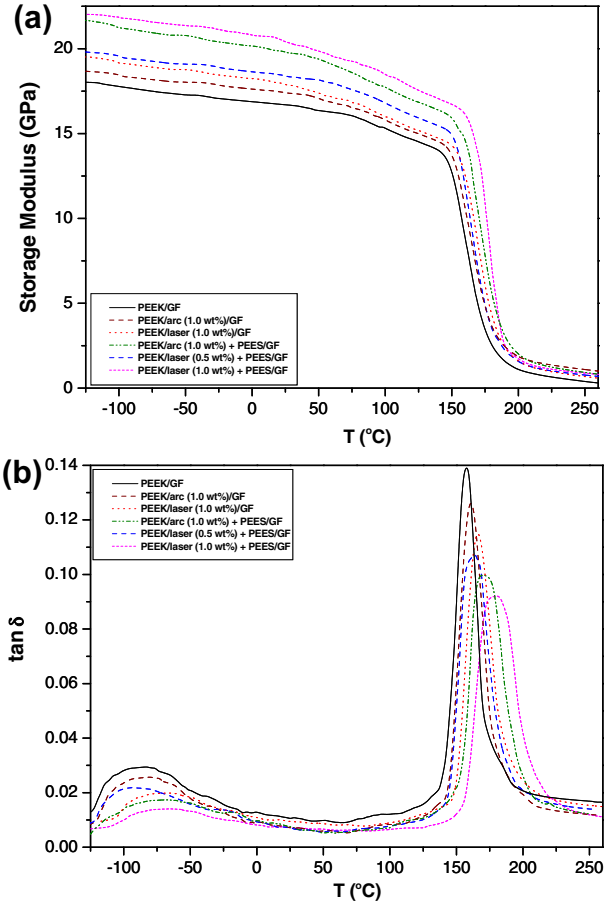

Fig. 7 – Evolution of the storage modulus E' (a) and tan δ (b) as a function of temperature, at a frequency of 1 Hz, for the PEEK/SWCNT/glass fiber laminates.

to have detrimental effects on fiber impregnation [17]. As mentioned, the gaps within the glass fiber tows are of the order of 1–2 μm. Therefore, it is more difficult for the non-wrapped nanotubes to penetrate within the fiber tows. In the areas where the fiber tows are surrounded by large CNT bundles there would be weaker interfacial adhesion between the matrix and the glass fibers, as well as slightly higher internal porosity, resulting in a lower E'. On the other hand, enhanced modulus is systematically obtained for composites incorporating laser-grown SWCNTs in comparison to those with arc-purified SWCNTs. With regards to the CNT content, samples including 1.0 wt% loading have ~10% higher modulus than those with 0.5 wt%; further increase would be expected if more SWCNTs could be uniformly incorporated into the matrix.

Our experimental data reveal a substantial drop in the storage modulus of all the laminates between 150 and 200 °C, an interval which corresponds to the glass transition of the composites. At higher temperatures, only small differences are found between E' of samples with wrapped and non-wrapped SWCNTs, which could be due to a decoupling of the compatibilizing layer. However, the relative increment in modulus versus the control PEEK/GF rises with increasing temperature. Thus, at 200 °C, 1.0 wt% wrapped arc-SWCNTs raise the modulus by ~75%. This indicates that the stiffening

Table 3 – Storage modulus E' at 25, 100 and 200 °C, glass transition temperature T_g, tan δ maximum value and width at half maximum β for the different PEEK laminates, obtained from dynamic mechanical analysis measurements at a frequency of 1 Hz.

Sample (% SWCNTs)	$E'_{25°C}$ (GPa)	$E'_{100°C}$ (GPa)	$E'_{200°C}$ (GPa)	T_g (°C)	tan δ_{max} (a.u.)	β (°C)
PEEK	3.8 ± 0.1	3.3 ± 0.1	0.43 ± 0.02	148.0 ± 0.5	0.172 ± 0.004	17 ± 1
PEEK/GF	16.7 ± 0.6	15.3 ± 0.5	1.14 ± 0.04	157.8 ± 0.8	0.139 ± 0.005	20 ± 1
PEEK/arc (1.0 wt%)/GF	17.5 ± 0.3	15.8 ± 0.4	1.83 ± 0.05	160.7 ± 0.8	0.128 ± 0.006	22 ± 1
PEEK/laser (1.0 wt%)/GF	18.0 ± 0.5	16.0 ± 0.6	1.55 ± 0.03	165.2 ± 0.6	0.117 ± 0.003	26 ± 2
PEEK/laser (0.5 wt%) + PEES/GF	18.4 ± 0.4	16.8 ± 0.3	1.57 ± 0.05	163.3 ± 0.9	0.108 ± 0.003	23 ± 1
PEEK/arc (1.0 wt%) + PEES/GF	19.8 ± 0.3	17.7 ± 0.2	2.01 ± 0.06	171.9 ± 0.9	0.101 ± 0.004	28 ± 2
PEEK/laser (1.0 wt%) + PEES/GF	20.3 ± 0.2	18.4 ± 0.1	1.70 ± 0.04	178.1 ± 0.7	0.093 ± 0.002	33 ± 1

effect is more pronounced above the softening point of the matrix, which could be explained considering that the modulus of the SWCNTs changes only slightly with temperature [45]. These results are consistent with DMA studies of vapor-grown carbon nanofiber (CNF)/PEEK [24] composites prepared by injection molding, which show higher relative increase in the matrix stiffness above than below the T_g.

The evolution of tan δ (ratio of the loss to storage modulus, a measure of the damping within the system) as a function of temperature (Fig. 7b) exhibits two relaxation peaks: the maximum at lower temperatures (β relaxation) is associated with local motions of the ketone groups, and the most intense peak (α relaxation) corresponds to the T_g; these data are collected in Table 3. T_g of the laminates differ from that of pure PEEK (~148 °C [25]) since this transition temperature is sensitive to interfacial interactions between the polymer and the reinforcements both at the microscale and nanoscale [13]. The inclusion of fillers decreases the free volume and restricts the mobility of the PEEK chains, which is reflected in higher T_g values. Thus, T_g increases by ~10 °C with the addition of the GF, in agreement with results reported for other GF-reinforced thermoplastics such as PC [44], polypropylene (PP) or poly(lactic acid) (PLA) [46]. The presence of the SWCNTs, which are dimensionally similar to the polymer segment units, more efficiently hinders the chain motion, thereby leading to larger temperature increments. These results are consistent with the behavior found by Warrier et al. [13] for epoxy/glass fiber/CNT, where composites with CNTs dispersed in the matrix showed enhanced T_g in comparison with binary epoxy/glass fiber samples. With increasing CNT loading, the restriction in mobility becomes stronger, resulting in a higher transition temperature. Regarding the different laminates, higher values are systematically found for composites incorporating polysulfone in comparison to non-compatibilized composites. The addition of 1.0 wt% arc and laser-grown SWCNTs dispersed in PEES raises the T_g of the reference by about 14 and 20 °C, respectively, whereas the same amounts of non-wrapped SWCNTs only lead to increments of 3 and 7 °C. These results are in very good agreement with those obtained from DSC thermograms. The significant T_g enhancement in the compatibilized systems is attributed to the high T_g of the amorphous polysulfone combined with the strong restrictions on polymer chain motion induced by the improved adhesion between the matrix and nanofiller phases. In contrast, the non-compatiblized samples show a smaller increase, probably due to partial agglomeration of the SWCNTs at the fiber interface. The agglomerates could alter the flow behavior of the matrix during impregnation, resulting in nanometer scale porosities [17]; this leads to an increase in the free volume between the polymer molecules, allowing additional mobility, which may explain their lower T_g.

The damping in the transition region measures the amount of energy used to deform the material that is directly dissipated into heat. In comparison with pure PEEK [25], the height of tan δ peak decreases in the presence of the glass fiber, since the interfacial adhesion fiber–matrix hinders the molecular movement. Moreover, the incorporation of the SWCNTs leads to an additional reduction in tan δ_{max}, indicating that the mechanical loss to overcome friction between molecular chains decreases after adding the nanofillers. The reduction in tan δ_{max} height is systematically more pronounced for the compatibilized samples (Table 3), being about 35% for the laminate including 1.0 wt% wrapped laser SWCNTs in comparison to the reference composite. This also reflects the more effective immobilization caused by the SWCNTs dispersed in PEES. Moreover, as mentioned earlier, the compatibilized samples exhibit better fiber impregnation, another factor that contributes to enhancement of the restriction effect. On the other hand, the broadening of the tan δ peak can also be interpreted as enhanced filler–matrix interactions. The CNTs and fibers disturb the relaxation of adjacent polymer chains, which would behave differently from those situated in the bulk matrix, resulting in a wider peak. The data for width at half maximum value (β) for PEEK and the different laminates are collected in Table 3. β of pure PEEK is about 18 °C and increases slightly (~2 °C) with the incorporation of the fibers. The broadening is more pronounced for composites including SWCNTs, in particular those incorporating PEES. Thus, for the laminate including 1.0 wt% laser SWCNTs dispersed in the compatibilizer, β is around 33 °C. The aforementioned effect has been previously reported for PEEK/CNF composites [24] and was attributed to a more inhomogeneous amorphous phase in the composites in relation to the pure matrix. It is worthy to note that the trends observed from the DMA spectra of the different laminates are consistent with those described previously for PEEK/SWCNT and PEEK/SWCNT + PEES composites [28], where the compatibilized samples, in particular those including laser-grown CNTs, exhibited the highest E' and T_g values. These results

indicate that the incorporation of a compatibilizer with high T_g and dual affinity with the matrix and the nanofillers enhances the dynamic mechanical properties of PEEK/GF composites.

3.7. *Tensile and flexural properties*

The static mechanical properties of the laminates were also investigated, and typical room temperature stress–strain curves are shown in Fig. 8. The in-plane tensile modulus and strength as well as the corresponding flexural properties are plotted in Fig. 9. The summary of the mechanical test results is collected in Table 4. The tensile Young's modulus (E) and flexural modulus (E_f) of pure PEEK (~4.1 and 4.3 GPa, respectively) experience about 2.8 and 3.0-fold enhancement with the addition of the glass fiber, consistent with previous literature values for glass fiber-reinforced PEEK [22]. Further inclusion of the SWCNTs results in remarkable improvements in the flexural modulus of the binary composite, while the in-plane Young's modulus only increases moderately. The incorporation of 1.0 wt% wrapped arc and laser-SWCNTs raises E_f by about 29% and 33%, respectively, whilst the increments in E are significantly lower, around 14% and 16%. For multiscale composites, it is expected that the nanoscale reinforcement mostly influences the properties that are matrix-dominated. The noticeable increase in the flexural modulus with the inclusion of the nanofillers is attributed to the reinforcement effect of the SWCNTs in the z-direction, since the flexural properties are mainly matrix-dominated. However, a moderate increase is achieved in the longitudinal Young's modulus, which is fiber-dominated. These observations are in agreement with the behavior reported for epoxy/MWCNT/glass fiber laminates [8], where the inclusion of MWCNTs significantly enhanced the mechanical properties out-of-plane, whereas those in-plane only improved marginally. Concerning the different laminates, the highest increments are again found for those including PEES. Thus, the flexural moduli of composites with wrapped arc and laser-grown SWCNTs are on average 20% higher than the corresponding non-compatibilized samples. Qualitatively similar behavior, albeit with

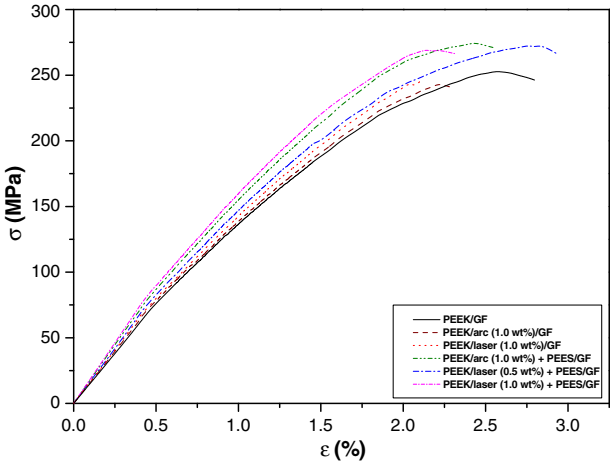

Fig. 8 – Representative stress–strain curves at room temperature obtained from tensile tests of PEEK based laminates.

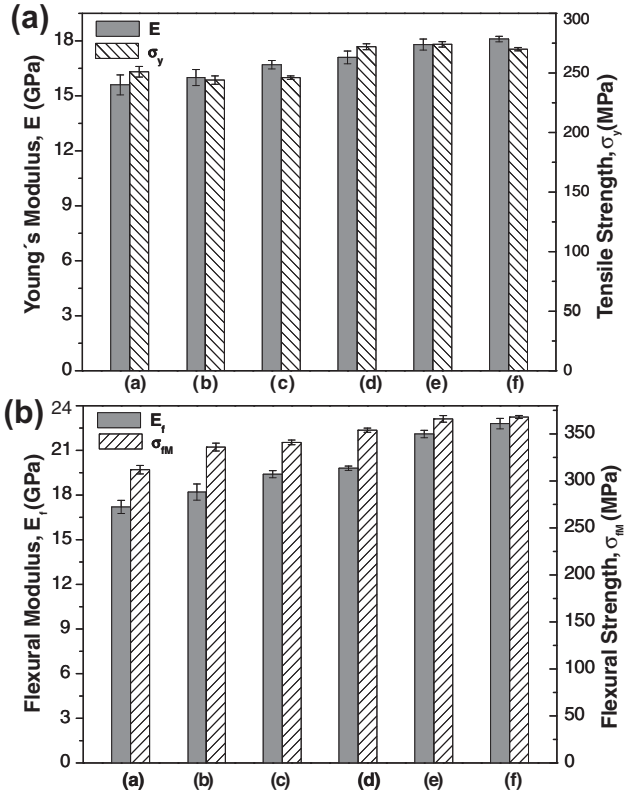

Fig. 9 – Mechanical properties of PEEK/SWCNT/glass fiber laminates: (a) in-plane Young's modulus and tensile strength; (b) flexural modulus and strength. The indicated samples are: (a) PEEK/glass fiber; (b) PEEK/arc (1.0 wt%)/glass fiber; (c) PEEK/laser (1.0 wt%)/glass fiber; (d) PEEK/laser (0.5 wt%) + PEES/glass fiber; (e) PEEK/arc (1.0 wt%) + PEES/glass fiber; (f) PEEK/laser (1.0 wt%) + PEES/glass fiber.

smaller differences was observed for E values. The larger increase in the moduli of the compatibilized systems probably results from enhanced matrix-nanotube load transfer, induced by improved dispersion and stronger interfacial bonding. Moreover, the laminates including PEES exhibit slightly lower internal porosity than those non-compatibilized, due to the absence of CNT agglomerates, which could also contribute to the improvement in the mechanical behavior. Nevertheless, since the differences in void content are fairly small, the enhancement in properties attained should be mostly ascribed to the more effective reinforcement effect due to the addition of the compatibilizer. Kim et al. [47] reported the tensile and flexural properties of CNT-modified carbon fiber-reinforced epoxy composites, and found that the degree of CNT dispersion strongly influenced the matrix-dominated mechanical properties; longer sonication times for CNT dispersion had a positive effect on the final flexural properties of the multiscale composites. On the other hand, the mechanical properties seem to be only slightly influenced by the quality of the nanofillers; the increments in the flexural and Youngś moduli attained with the inclusion of laser-grown CNTs are on average 5% and 3% higher than those achieved with similar amounts of arc-purified SWCNTs. With regards to the CNT content, it is found that the improvements in E_f

Table 4 – Room temperature tensile, flexural and Charpy notched impact tests results for the different laminates: Young's modulus (E), tensile strength at yield (σ_y), strain at break (ε_b), flexural modulus (E_f) , flexural strength (σ_{fM}) and impact strength (G).

Sample (% SWCNTs)	E (GPa)	σ_y (MPa)	ε_b (%)	E_f (GPa)	σ_{fM} (MPa)	G (kJ/m^2)
PEEK	4.1 ± 0.1	125 ± 1	12.3 ± 0.4	4.3 ± 0.1	170 ± 1	6.0 ± 1
PEEK/GF	15.6 ± 0.5	251 ± 4	2.8 ± 0.1	17.2 ± 0.4	312 ± 4	8.0 ± 1
PEEK/arc (1.0 wt%)/GF	16.0 ± 0.4	244 ± 3	2.2 ± 0.2	18.2 ± 0.5	336 ± 4	7.5 ± 0.9
PEEK/laser (1.0 wt%)/GF	16.7 ± 0.2	246 ± 1	2.0 ± 0.1	19.4 ± 0.2	341 ± 2	7.7 ± 0.8
PEEK/laser (0.5 wt%) + PEES/GF	17.1 ± 0.3	272 ± 2	2.9 ± 0.2	19.8 ± 0.1	354 ± 2	9.0 ± 0.7
PEEK/arc (1.0 wt%) + PEES/GF	17.8 ± 0.3	274 ± 2	2.6 ± 0.1	22.1 ± 0.2	366 ± 3	8.6 ± 0.8
PEEK/laser (1.0 wt%) + PEES/GF	18.1 ± 0.1	270 ± 1	2.3 ± 0.1	22.8 ± 0.3	368 ± 1	8.8 ± 0.6

and E for 1.0 wt% loading (~33% and 16%, respectively) are about double than those attained with 0.5 wt% (~15% and 9%).

The tensile strength (σ_y) and flexural strength (σ_{fM}) of pure PEEK (~125 and 170 MPa, respectively) increase by about 100% and 85% with the inclusion of the glass fiber. Regarding the compatibilized laminates, the trends observed are similar to those described previously for the corresponding moduli, albeit the variations in comparison with the reference composite are smaller (~18% and 16% for 1.0 wt% arc and laser-grown SWCNTs, respectively), indicating that the wrapped nanofillers are more effective in enhancing the stiffness than the strength of the matrix. In contrast, the addition of non-wrapped SWCNTs has negligible effect on the tensile strength of PEEK/glass fiber, and the flexural strength only improves marginally.

For polymer/CNT/fiber multiphase composites, E can be predicted with a two-phase model. Firstly, taking reported data for the modulus (~1 TPa) of SWCNTs [48], the corresponding values of polymer/CNT composites can be calculated according to the Krenchel's rule of mixtures for discontinuous reinforcement [49]; since the CNTs are not perfectly stretched when dispersed in a polymer matrix, a decreased shape factor (1/5) should be considered [50]. The polymer/CNT mixture can then be regarded as a new matrix phase and the fibers as the filler phase; the rule of mixtures can be subsequently used to calculate the Youngs modulus of the laminates: $E_c = \zeta_E V_f E_f + (1 - V_f)E_m$, where ζ_E is the fiber efficiency factor (~0.5 for continuous bidirectional fibers [51]), E_f and E_m are the fiber and matrix modulus, respectively, and V_f the fiber volume fraction. Considering the high modulus (~73 GPa) of the glass fiber [52], the calculated modulus for laminates including 1.0 wt% SWCNTs is ~20.5 GPa, between 13% and 27% higher than the measured data. The discrepancies between experimental and theoretical values probably arise from several factors such as the waviness of the glass fiber, which decreases its effective Youngs modulus, and the very high viscosity of the resin, that precludes complete glass fiber wetting; hence the fibers are not able to express their full capability for stiffness enhancement. In these multiscale composites, the main requirements for effective reinforcement are good CNT dispersion and interfacial stress transfer. This latter factor is probably the most crucial issue. The stress is only efficiently transferred if there is good interfacial bonding between the matrix and the two filler phases. Despite the fact that the compatibilizer improves the dispersion of the SWCNTs and their interaction with the matrix, these still remain gathered in small bundles, as revealed by SEM micrographs, and shear slippage of individual nanotubes within the bundle may occur, thereby limiting stress transfer. Moreover, the formation of bundles and the small defects that may be present at the SWCNT surface would reduce their effective Young's modulus. Thus, the values obtained are somewhat lower than predicted by the rule of mixtures, which is an upper bound expected in the case of perfect CNT dispersion and adhesion to the matrix, perfect fiber–matrix bonding and zero inter-tow gap.

On the other hand, the incorporation of the fillers strongly affects the elongation at break (ε_b) of the matrix. This parameter (~12% for pure PEEK) falls drastically with the addition of the glass fiber (nearly 80%, see Table 4), which is understandable considering that the high volume of rigid fillers obstructs the drawing process of the matrix, restricting its extent of plastic deformation. This is the typical behavior found in glass fiber-reinforced thermoplastics [22,44]. Regarding the various laminates, lower ε_b is found for samples including non-wrapped nanofillers. This indicates that the incorporation of the polysulfone reduces stress concentrations at the polymer-nanotube interface, thereby improving the matrix ductility. Similar trends were observed from the previous comparative study of PEEK/SWCNT composites with and without compatibilizer [28], thereby confirming the effective role of the polysulfone. The drawing process should be considerably more limited in composites including non-wrapped SWCNTs due to the presence of small CNT agglomerates, which strongly restrict plastic deformation of the matrix. These results are consistent with the observations from our previous work [28], which indicated that secondary cracks nucleate at the same time from numerous regions with small CNT aggregates and eventually coalesce, leading to premature failure. On the other hand, it is clear that ε_b decreases with increasing CNT content. Thus, the laminate reinforced with 0.5 wt% wrapped laser-grown CNTs shows similar ultimate strain as the reference material, whilst it decreases about 18% for the sample including 1.0 wt% loading. As the concentration rises, it is more difficult to perfectly disperse the CNT bundles within the polymer matrix, even in the presence of the compatibilizer.

In order to obtain more information regarding the failure in flexural tests, fractured surfaces have been examined by SEM (Fig. 10). For all the samples, fiber fracture dominates

the failure mechanism combined with resin yielding at the fracture zone. This suggests that tensile stresses are the main cause for failure [53]. As it can be observed, CNT pull-out instead of CNT breaking is the result of flexural deformation in PEEK/SWCNT/glass fiber composites; crack propagation is retarded by the pulling force of the CNTs at the crack surface, due to an energy dissipation phenomenon. This increases the delamination resistance in comparison to the reference laminate. In the case of the non-compatibilized sample (Fig. 10a and b), after the rupture of the specimen only a few SWCNTs are found to protrude out of the matrix. On the other hand, the micrographs corresponding to the compatibilized laminate (Fig. 10c and d) clearly show several SWCNTs pulled-out of the matrix. Moreover, some SWCNTs can be observed at the matrix-fiber interface (Fig. 10c), extending into the surrounding matrix, which is likely to stiffen the matrix and provide increased lateral support for the load-bearing microscale fibers. Therefore, SWCNTs wrapped in the compatibilizer seem to be more effective for increasing the failure load, leading to improved flexural properties. This improvement is probably attributed to a stiffer CNT-reinforced matrix and/or enhanced fiber–matrix interfacial interactions [7].

3.8. *Charpy impact strength*

To evaluate the toughness of the laminates, room temperature Charpy notched impact tests were performed, and the quantitative results obtained are included in Table 4. The impact strength of neat PEEK (~6 kJ/m^2) increases by about 33% with the addition of the glass fiber. Further addition of the CNTs results in only small changes in the specimen toughness. Thus, the inclusion of 1.0 wt% non-wrapped arc and laser-SWCNTs decreases the impact strength by 6% and 4%, respectively, in comparison with the reference laminate, whereas the addition of similar amounts of SWCNTs dispersed in PEES increases it by an average of 8%. The composite reinforced with 0.5 wt% wrapped laser-grown SWCNTs has the best impact strength, about 13% higher than the reference laminate. There are several factors controlling the impact strength of reinforced composites [54]; one is a diminishing effect of the fillers on the toughness due to a drastic decrease in the elongation at break and hence a reduction of the area under the stress–strain curves. In addition, new stress concentrations will be formed around the filler ends, area of poor adhesion, and region of filler aggregation. Other is a positive effect due to the fact that the fillers reduce the crack propagation rate by forcing cracks to go around them. Moreover, the increase of fracture resistance is the result of energy-dissipating mechanisms based on fiber bridging (the cracked matrix is bridged by intact and/or failed fibers, which debond, slip and pull-out). The net effect depends on the competition of these factors. Comparing the experimental results for pure PEEK and the control laminate, it is obvious that the reducing effect of the glass fiber on crack propagation rate dominates, leading to an increase in the impact strength. This behavior is in agreement with the enhancement in the impact strength reported for other thermoplastic/glass fiber composites based on PLA and PP matrices [46].

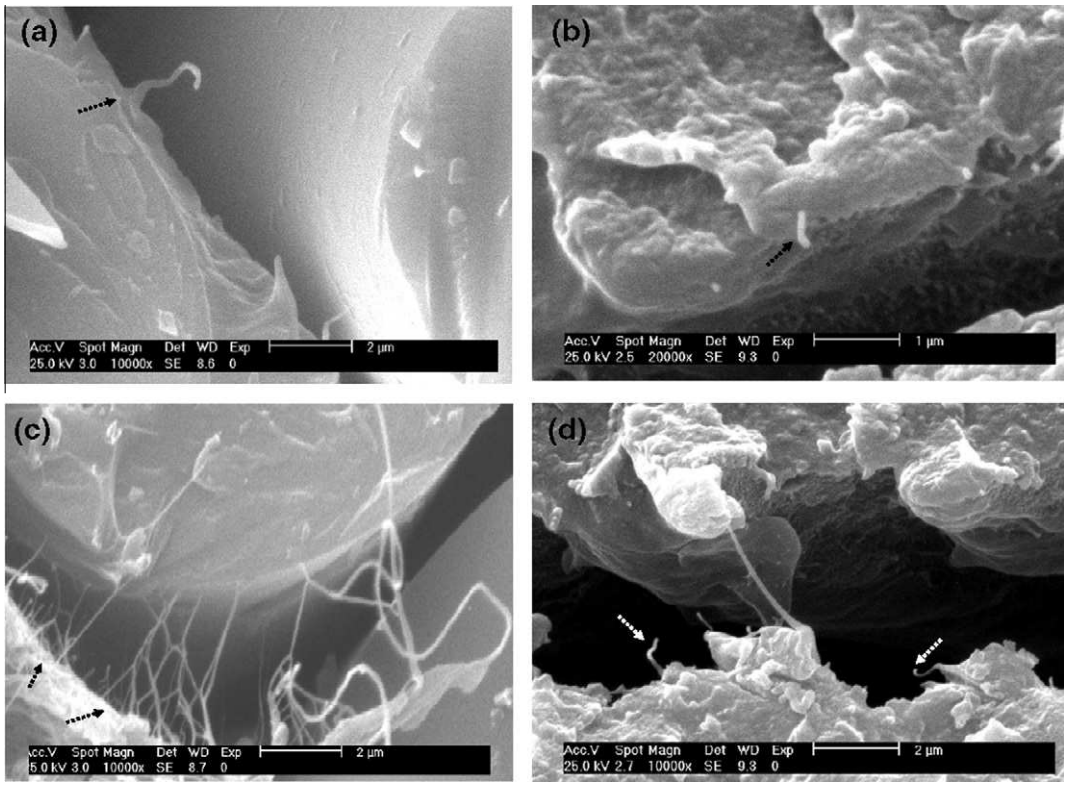

Fig. 10 – SEM micrographs from fractured surfaces of flexural specimens: (a) and (b) PEEK/laser (1.0 wt%)/glass fiber; (c) and (d) PEEK/laser (1.0 wt%) + PEES/glass fiber. (a) and (c) were taken from a region adjacent to the fiber tows, whilst (b) and (c) correspond to matrix-rich areas. The dashed arrows point out SWCNTs pulled-out of the matrix.

Regarding the laminates including SWCNTs, the toughness seems to be sensitive to the size, state of dispersion of the nanofillers and their interfacial adhesion with the matrix. The non-compatibilized samples incorporating 1.0 wt% SWCNT loading have small agglomerates, which serve as stress concentration sites that promote the formation of dimples and nucleate cracks. This aggravates the brittleness under high strain rates, resulting in a small decrease of the impact strength and premature system failure in comparison with the reference composite. However, the toughness improves moderately by the addition of the compatibilizer, which can be ascribed to a more homogeneous nanofiller dispersion which minimizes the stress concentration nuclei, as well as an enhanced CNT-matrix interfacial adhesion, that provides an effective barrier for pinning and bifurcation of the advancing cracks. Similar trends were found for the comparison of the toughness of compatibilized and non-compatiblized PEEK/SWCNT composites, albeit quantitatively larger improvements in toughness were attained by the addition of the polysulfone. With respect to the influence of the nanofiller type and concentration, it was found that the laminate including 0.5 wt% wrapped laser-grown SWCNTs had the highest impact strength, probably due to the synergic effect of higher quality than arc-purified SWCNTs and the absence of agglomerates, which minimize the presence of nanoscale pores.

Overall, the mechanical tests performed confirm that although the SWCNTs constitute a very small weight fraction of the laminate as a whole, they are able to modify the macroscopic mechanical properties; the developed multiscale composites incorporating polysulfone demonstrate significantly improved behavior versus the reference PEEK/glass fiber, showing simultaneous increases in stiffness, strength and toughness. This investigation opens up new perspectives for the development of engineering multifunctional materials to be used in structural applications, particularly for the aerospace and automotive industries.

4. Conclusions

In the present work, the thermal, electrical and mechanical properties of PEEK/SWCNT/glass fiber laminates including polysulfone as a compatibilizer have been investigated and compared with the behavior of composites incorporating similar non-wrapped nanofillers. Morphological observations revealed a more uniform CNT distribution for the compatibilized laminates. DSC thermograms indicated a slight decrease in the crystallization temperature and degree of crystallinity of PEEK for both compatibilized and non-compatibilized composites, attributed to the restrictions on polymer chain mobility imposed by the nanofillers. However, no significant changes were observed in the melting behavior of the polymer. TGA studies showed a remarkable thermal stability enhancement in the presence of the polysulfone. The incorporation of wrapped SWCNTs resulted in a strong increase in the thermal conductivity of the polymer. The laminates show anisotropic behavior; the electrical conductivity out-of-plane turned out to be about one order of magnitude lower than the in-plane. DMA experiments demonstrated a strong increase in both the storage modulus and glass transition temperature of the compatibilized composites in comparison to PEEK/glass fiber. The addition of wrapped nanofillers led to a significant improvement in the out-of-plane mechanical properties (e.g. flexural modulus and strength), whilst the tensile properties increased moderately, due to the dominating effect of the fiber-reinforcement. The longitudinal Young's modulus of non-compatibilized composites increased very modestly, and their flexural properties improved only marginally. Overall, the mechanical tests demonstrated simultaneous enhancements in stiffness, strength and toughness by the inclusion of SWCNTs dispersed in polysulfone. Improved properties were found for laminates reinforced with laser-grown SWCNTs. The tests performed confirm that the addition of wrapped SWCNTs to conventional thermoplastic/glass fiber composites leads to new high-performance multifunctional materials suitable for a wide range of applications.

Acknowledgments

Financial support from a coordinated project between the National Research Council of Canada (NRC) and the Spanish National Research Council (CSIC) is gratefully acknowledged. Dr. A. Diez would like to thank the Spanish Ministry of Science and Innovation (MICINN) for the Juan de la Cierva postdoctoral contract. Mr. González-Domínguez acknowledges the FPU predoctoral fellowship granted by MICINN.

REFERENCES

[1] Qiu J, Zhang C, Wang B, Liang R. Carbon nanotubes integrated multifunctional and multiscale composites. Nanotechnology 2007;17:275708–11.
[2] Marsh G. Next step for automotive materials. Mater Today 2003;6:36–43.
[3] Brondsted P, Lilholt H, Lystrup A. Composite materials for wind power turbine blades. Annu Rev Mater Res 2005;35:505–38.
[4] Moritis G. Hub. New technologies provide access to more deepwater reserves. Oil Gas J 2003;101:54–61.
[5] Cecen V, Sarikanat M, Seki Y, Govsa T, Yildiz H, Tavman IH. Polyester composites reinforced with noncrimp stitched carbon fabrics: mechanical characterization of composites and investigation on the interaction between polyester and carbon fiber. J Appl Polym Sci 2006;102(5):4554–64.
[6] Thostenson ET, Ren Z, Chou T-W. Advances in the science and technology of carbon nanotubes and their composites: a review. Compos Sci Technol 2001;61(13):1899–912.
[7] Qian H, Greenhalgh ES, Shaffer MSP, Bismarck A. Carbon nanotube-based hierarchical composites: a review. J Mater Chem 2010;20:4751–62.
[8] Gojny FH, Wichmann MHG, Fiedler B, Bauhofer W, Schulte K. Influence of nano-modification on the mechanical and electrical properties of conventional fiber-reinforced composites. Composites A 2005;36:1525–35.
[9] Garcia EJ, Hart AJ, Wardle BL, Yamamoto N. Fabrication and multifunctional properties of hybrid laminate with aligned carbon nanotubes grown in situ. Compos Sci Technol 2008;68:2034–41.
[10] Bekyarova E, Thostenson ET, Yu A, Kim H, Gao J, Tang J, et al. Multiscale carbon nanotube–carbon fiber reinforcement for advanced epoxy composites. Langmuir 2007;23:3970–4.

[11] Yokozeki T, Iwahori Y, Ishiwata S. Matrix cracking behaviors in carbon fiber/epoxy laminates filled with cup-stacked carbon nanotubes (CSCNTs). Composites A 2007;38:917–24.
[12] Barber AH, Zhao Q, Wagner HD, Baillie CA. Characterization of E-glass-propylene interfaces using carbon nanotubes as strain sensors. Compos Sci Technol 2004;64(13–14):1915–9.
[13] Warrier A, Godara A, Rochez O, Mezzo L, Luizi F, Gorbatikh L, et al. The effect of adding carbon nanotubes to glass/epoxy composites in the fibre sizing and/or the matrix. Composites A 2010;41:532–8.
[14] Wichmann MHG, Sumfleth J, Gojny FH, Quaresimin M, Fiedler B, Schulte K. Glass-fibre-reinforced composites with enhanced mechanical and electrical properties – benefits and limitations of a nanoparticle modified matrix. Eng Fract Mech 2006;73:2346–59.
[15] Qiu JJ, Zhang C, Wang B, Liang R. Carbon nanotube integrated multifunctional multiscale composites. Nanotechnology 2007;18:275708–11.
[16] Sadeghian R, Gangireddy S, Minaie B, Hsiao KT. Manufacturing carbon nanofibers toughened polyester/glass fiber composites using vacuum assisted resin transfer molding for enhancing the mode-I delamination resistance. Composites A 2006;37:1787–95.
[17] Fan Z, Hsiao K-T, Advani SG. Experimental investigation of dispersion during flow of multi-walled carbon nanotube-polymer suspension in fibrous porous media. Carbon 2004;42(4):871–6.
[18] Staniland PA. Poly(ether ketone)s. In: Allen G, Bevington JC, editors. Comprehensive polymer science, vol. 5. New York: Pergamon Press; 1989. p. 484–97.
[19] Searle OB, Pfeiffer RH. Victrex® poly(ethersulfone) (PES) and Victrex® poly(ether ether ketone) (PEEK). Polym Eng Sci 1985;25(8):474–6.
[20] Sarasua JR, Remiro PM, Pouyet J. Effects of thermal history on mechanical behavior of PEEK and its short-fiber composites. J Mater Sci 1995;30:3501–8.
[21] Sınmazçelik TST, Yılmaz T. Thermal aging effects on mechanical and tribological performance of PEEK and short fiber reinforced PEEK composites. Mater Des 2007;28(2):641–8.
[22] Davim JP, Reis P, Lapa V, Conceição CA. Machinability study on polyetheretherketone (PEEK) unreinforced and reinforced (GF30) for applications in structural components. Compos Struct 2003;6(1):67–73.
[23] Katsiropoulos ChV, Pantelakis SpG, Meyer BC. Mechanical behaviour of non-crimp fabric PEEK/C thermoplastic composites. Theor Appl Fract Mech 2009;52:122–9.
[24] Sandler J, Werner P, Shaffer MSP, Demchuck V, Altstadt V, Windle AH. Carbon-nanofibre-reinforced poly(ether ether ketone) composites. Composites A 2002;33:1033–9.
[25] Díez-Pascual AM, Naffakh M, Gómez MA, Marco C, Ellis G, Gónzalez-Domínguez JM, et al. Development and characterization of PEEK/carbon nanotube composites. Carbon 2009;47(13):3079–90.
[26] Díez-Pascual AM, Naffakh M, Gómez MA, Marco C, Ellis G, Gónzalez-Domínguez JM, et al. Influence of a compatibilizer on the thermal and dynamic mechanical properties of PEEK/carbon nanotube composites. Nanotechnology 2009;20:315707–20.
[27] Díez-Pascual AM, Naffakh M, Gónzalez-Domínguez JM, Anson A, Martinez-Rubi Y, Simard B, et al. High-performance PEEK/carbon nanotube composites compatibilized with polysulfones. I – Structure and thermal properties. Carbon 2010;48(12):3485–99.
[28] Díez-Pascual AM, Naffakh M, Gónzalez-Domínguez JM, Anson A, Martinez-Rubi Y, Simard B, et al. High-performance PEEK/carbon nanotube composites compatibilized with polysulfones. II – Mechanical and electrical properties. Carbon 2010;48(12):3500–11.
[29] Begeman ML, Amstead BH. Annual book of ASTM standards, vol. 8. Philadelphia: ASTM Publishers. 1989. p. 386–7.
[30] Blundell DJ, Osborn BN. The morphology of poly(aryl-ether-ether-ketone). Polymer 1983;24(8):953–8.
[31] Parker WJ, Jenkins RJ, Butler CP. Flash method of determining thermal diffusivity specific heat and thermal conductivity. J Appl Phys 1961;32(12):1679–84.
[32] Jin J, Song M, Pan F. A DSC study of the effect of carbon nanotubes on crystallization behaviour of poly(ethylene oxide). Thermochim Acta 2007;456:25–31.
[33] Meng H, Sui GX, Fang PF, Yang R. Effects of acid- and diamine-modified MWNTs on the mechanical properties and crystallization behavior of polyamide 6. Polymer 2008;49:610–20.
[34] Moniruzzaman M, Winey KI. Polymer nanocomposites containing carbon nanotubes. Macromolecules 2006;39(16):5194–205.
[35] Markov A, Fiedler B, Schulte K. Electrical conductivity of carbon black/fibres filled glass-fibre reinforced thermoplastic composites. Composites A 2006;37:1390–5.
[36] Wang S, Qiu J. Enhancing thermal conductivity of glass fiber/polymer composites through carbon nanotubes incorporation. Composites B 2010;47(7):533–6.
[37] White CT, Todorov TN. Carbon nanotubes as long ballistic conductors. Nature 1998;393:240–2.
[38] Assael MJ, Antoniadis KD, Metaxa IN. Measurement of the enhancement of the thermal conductivity of an epoxy resin reinforced with glass fiber and carbon multiwalled nanotubes. J Chem Eng Data 2009;54:2365–70.
[39] Patton RD, Pittman Jr CU, Wang L, Hill JR. Vapor grown carbon fiber composites with epoxy and poly(phenylene sulfide) matrices. Composites A 1999;30:1081–91.
[40] Xu Y, Ray G, Abdel-Magid B. Thermal behavior of single-walled carbon nanotube polymer–matrix composites. Composites A 2006;37:114–21.
[41] Nan C-W, Liu G, Lin Y, Li M. Interface effect on thermal conductivity of carbon nanotube composites. Appl Phys Lett 2004;85:3549–51.
[42] Song L, Zhang H, Zhang Z, Xie S. Processing and performance improvements of SWNT paper reinforced PEEK nanocomposites. Composites A 2007;38(2):388–92.
[43] Shenogin S, Bodapati A, Xue L, Ozisik R, Keblinski P. Effect of chemical functionalization on thermal transport of carbon nanotube composites. Apply Phys Lett 2004;85:2229–31.
[44] Samakrut N, Krailas S, Rimdusit S. Characterization of short glass fiber-reinforced PC/ABS blends. J Met Mater Miner 2008;18(2):207–11.
[45] Lu JP. Elastic properties of carbon nanotubes and nanoropes. Phys Rev Lett 1997;79(7):1297–300.
[46] Huda MS, Drzal LT, Mohanty AK, Misra M. Chopped glass and recycled newspaper as reinforcement fibers in injection molded poly(lactic acid) (PLA) composites: a comparative study. Compos Sci Technol 2006;66:1813–24.
[47] Kim M, Park Y-B, Okoli O, Zhang C. Processing, characterization, and modeling of carbon nanotubes-reinforced multiscale composites. Compos Sci Technol 2009;69:335–42.
[48] Xie XL, Mai Y-W, Zhouet X-P. Dispersion and alignment of carbon nanotubes in polymer matrix: a review. Mat Sci Eng R 2005;49(4):89–112.
[49] Krenchel H. Fibre reinforcement. Copenhagen: Akademisk Forlag; 1964. p. 159–60.
[50] Fragneaud B, Masenelli-Varlot K, Gonzalez-Montiel A, Terrones M, Cavaillé JY. Mechanical behavior of polystyrene grafted carbon nanotubes/polystyrene nanocomposites. Compos Sci Technol 2008;68:3265–71.

[51] Hollaway LC. Handbook of polymer composites for engineers. Cambridge: Woodhead Publishing Ltd.; 2010. p. 44–5.
[52] Bapanapalli S, Nguyen BN. Prediction of elastic properties for curved fiber polymer composites. Polym Compos 2008;16:544–50.
[53] Birger S, Moshonov A, Kenig S. Failure mechanisms of graphite-fabric epoxy composites subjected to flexural loading. Composites 1989;20:136–44.
[54] Crosby JM, Drye TR. How fibers affect fracture behaviour of nylon-66 composites. Mod Plast 1986;63:74–84.